



UNIVERSITI KUALA LUMPUR ASSESSMENT BRIEF

COURSE DETAILS	
INSTITUTE	UniKL BRITISH MALAYSIAN INSTITUTE
COURSE NAME	ELECTRONIC DEVICES AND CIRCUITS
COURSE CODE	BEB24503
COURSE LEADER	DR MOHD AZRAIE MOHD AZMI
LECTURER	DR MOHD AZRAIE MOHD AZMI, MR HJ AHMAD BASRI ZAINAL
SEMESTER & YEAR	OCTOBER 2025

ASSESSMENT DETAILS	
TITLE/NAME	LAB 2
WEIGHTING	20%
DATE/DEADLINE	2 JANUARY 2026 5:00 P.M.
COURSE LEARNING OUTCOME(S)	CLO 2: Construct experimental investigations with appropriate techniques and resources of BJT Small Signal Circuits and Op-Amp Circuits (P4, PLO4).
INSTRUCTIONS	Perform the following tasks: 1. Submit the report individually as instructed by Course Lecturer. 2. All answers must be in English language only.

Student Name: AHMAD NAFIS BIN MOHD ZULKIFLI	ID: 51224125264	Group: L01-B01
Assessor's Comment:		Marks:

Verified by: Course Leader [MAZR] Prepared by: [MAZR] I hereby declare that all my team members have agreed with this assessment. All team members are certain that this assessment complies with the Course Syllabus. Signature:  MAZR Date : 2/10/2025	QSC format verification 	PC/HOS content validation  Ts. Dr. Zainil Livana binti Zahari Programme Coordinator BENET Electronics Technology Section Universiti Kuala Lumpur British Malaysian Institute
--	---	---

Instruction:

TASK NO	CLO	MARKING SCHEME	MARKS
1	2	Analysis and simulation of non-inverting amplifier circuit	20
2	2	Construct and test non-inverting amplifier circuit	30
3	2	Design and simulation of active filter circuit	30
4	2	Analysis & conclusion	20
		TOTAL	100



BEB24503 ELECTRONIC DEVICES AND CIRCUITS

LAB 2: OPERATIONAL AMPLIFIER

LECTURER: MR AHMAD BASRI

DATE: 2 JANUARY 2025

STUDENT NAME	STUDENT ID
AHMAD NAFIS BIN MOHD ZULKIFLI	51224125264

TABLE OF CONTENTS

1.0	Introduction.....	3
2.0	Objectives	4
3.0	Theory/Background	5
3.1	Active Filter and Cutoff Frequency	5
3.2	Types of Active Filters	5
3.3	Filter Order, Poles and Roll-Off Rate	6
3.4	Voltage Gain, Av and dB Scale	6
4.0	Procedure	7
4.1	Non-Inverting Op-Amp: Electrical Characteristics	7
4.1.1	Review of LM741 Datasheet	7
4.1.2	Voltage Gain and Power Bandwidth	8
4.1.3	Square-Wave Response and Slew Rate Measurement.....	10
4.1.2	Sine Wave with 0.5V at 30kHz.....	12
4.2	Construction and Testing of Non-Inverting Op-Amp Circuit.....	13
4.2.2	Square-Wave Response: Voltage Gain and Slew Rate.....	13
4.2.3	Sine Wave Response at 30kHz.....	14
3.3.1	Calculation to design a bandpass filter	15
3.3.2	Circuit Implementation based on Design Requirements	18
3.3.3	Simulation of Active Bandpass Filter (Buffered)	21
3.3.4	Comparison Table	24
5.0	Analysis.....	26
5.1	Working Principle of the Circuits	26
5.1.1	Working Principle of the Non-Inverting Amplifier.....	26
5.1.2	Working Principle of the Double-Pole Active Band-Pass Filter.....	26
5.2	Comparison Between Simulation and Practical Results (Non-Inverting Amplifier)	
	27	
5.3	Comparison Between Simulation Results and Design Requirements (Band-Pass Filter)	
	29	
5.4	Frequency Response Analysis.....	30
6.0	Conclusion	31

1.0 Introduction

Operational amplifier (op-amp) is one of the most popularly used device in electronics due to its versatility. The ideal op-amp possesses infinite voltage gain, infinite bandwidth, infinite input impedance and zero output impedance. Other characteristics of op-amp include Slew Rate, Common Mode Rejection Ratio (CMRR) and input offset voltage. There are many amplifier designs utilizing the properties of op-amp such as inverting and non-inverting amplifier circuits.

The op-amp is also popularly used in building active filter circuits. Many designs of low pass filter, high pass filter, notch filter and band pass filter are available. These circuits are simpler to design and easier to implement in comparison to its BJT counterpart.

2.0 Objectives

- a. To analyze and simulate electrical characteristics of a non-inverting op-amp circuit.
- b. To construct and test non-inverting amplifier circuit.
- c. To design active filter circuits within specific requirements.
- d. To investigate frequency response of the active filter circuit.

3.0 Theory/Background

For analysis purposes, op-amps are commonly assumed to be ideal, meaning they have infinite voltage gain, infinite input impedance, zero output impedance, zero input current, and infinite bandwidth. Under negative feedback conditions, the voltages at the inverting and non-inverting terminals are approximately equal ($V^- \approx V^+$). In practice, devices such as the LM741 exhibit non-ideal behavior, but still closely approximate ideal operation within their normal operating range, making them suitable for active filter applications.

3.1 Active Filter and Cutoff Frequency

Active filters are circuits that selectively pass signals within certain frequency ranges while attenuating signals outside those ranges. The frequency-selective behavior of active filters is determined by resistor–capacitor (RC) networks connected to the op-amp input.

The cutoff frequency f_c of an RC filter is defined as the frequency at which the output voltage magnitude drops to 70.7% (-3 dB) of the maximum value. For both low-pass and high-pass RC filters, the cutoff frequency is given by:

$$f_c = \frac{1}{2\pi RC}$$

where:

- R is the resistance in ohms (Ω)
- C is the capacitance in farads (F)

This equation is fundamental to the design of all active filters used in this laboratory.

3.2 Types of Active Filters

There are several common types of active filters:

- Low-Pass Filter (LPF): Allows signals with frequencies below the cutoff frequency to pass.
- High-Pass Filter (HPF): Allows signals with frequencies above the cutoff frequency to pass.
- Band-Pass Filter (BPF): Allows signals within a specific frequency band, between a lower cutoff frequency f_L and an upper cutoff frequency f_H , to pass.

In this experiment, a band-pass filter is implemented by cascading a high-pass filter and a low-pass filter.

3.3 Filter Order, Poles and Roll-Off Rate

The performance of an active filter is strongly influenced by the number of poles in the circuit. A pole corresponds to a single RC network. Each pole contributes a roll-off rate of:

$$20 \text{ dB/decade}$$

Thus:

- A single-pole filter has a roll-off rate of 20 dB/decade.
- A double-pole filter has a roll-off rate of 40 dB/decade.

To achieve a band-pass filter with a roll-off rate of ± 40 dB/decade, a double-pole high-pass filter and a double-pole low-pass filter are cascaded. This results in an overall fourth-order band-pass filter, which satisfies the laboratory requirements.

3.4 Voltage Gain, A_v and dB Scale

The voltage gain of an amplifier is defined as the ratio of output voltage to input voltage:

$$A_v = \frac{V_{out}}{V_{in}}$$

In frequency response analysis, gain is commonly expressed in decibels (dB). The conversion from voltage gain ratio to decibels is given by:

$$A_v(\text{dB}) = 20 \log_{10} \left(\frac{V_{out}}{V_{in}} \right)$$

This relationship is used in the AC sweep analysis to evaluate filter performance. A gain of **0** dB corresponds to unity gain ($V_{out} = V_{in}$), which represents the desired midband gain for this laboratory's band-pass filter.

4.0 Procedure

4.1 Non-Inverting Op-Amp: Electrical Characteristics

This task investigates the electrical characteristics of a non-inverting operational amplifier through simulation and analysis. Figure 1 shows the non-inverting LM741 operational amplifier circuit used in this experiment.

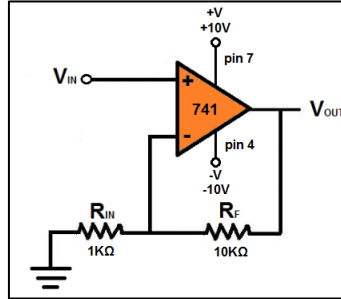


Figure 1: Non-inverting LM741 op-amp configuration.

4.1.1 Review of LM741 Datasheet

The specification sheet for the LM741 operational amplifier was downloaded and reviewed from the manufacturer's website. Important parameters related to the amplifier's performance were identified and highlighted, including slew rate (SR), common-mode rejection ratio (CMRR), input offset voltage and input impedance shown in Figure 2.

Texas Instruments		LM741					
www.ti.com		SNOSC25D – MAY 1998 – REVISED OCTOBER 2015					
6.5 Electrical Characteristics, LM741⁽¹⁾							
PARAMETER		TEST CONDITIONS		MIN	TYP	MAX	UNIT
Input offset voltage		$R_S \leq 10 \text{ k}\Omega$	$T_A = 25^\circ\text{C}$ $T_{A\text{MIN}} \leq T_A \leq T_{A\text{MAX}}$	1	5	mV	
				6		mV	
Input offset voltage adjustment range		$T_A = 25^\circ\text{C}, V_S = \pm 20 \text{ V}$		± 15		mV	
Input offset current		$T_A = 25^\circ\text{C}$ $T_{A\text{MIN}} \leq T_A \leq T_{A\text{MAX}}$		20	200	nA	
		$T_A = 25^\circ\text{C}$ $T_{A\text{MIN}} \leq T_A \leq T_{A\text{MAX}}$		85	500	nA	
Input bias current		$T_A = 25^\circ\text{C}$ $T_{A\text{MIN}} \leq T_A \leq T_{A\text{MAX}}$		80	500	nA	
Input resistance		$T_A = 25^\circ\text{C}, V_S = \pm 20 \text{ V}$			1.5	μA	
Input voltage range		$T_{A\text{MIN}} \leq T_A \leq T_{A\text{MAX}}$		± 12	± 13	V	
Large signal voltage gain		$V_S = \pm 15 \text{ V}, V_O = \pm 10 \text{ V}, R_L \geq 2 \text{ k}\Omega$	$T_A = 25^\circ\text{C}$ $T_{A\text{MIN}} \leq T_A \leq T_{A\text{MAX}}$	50	200	V/mV	
				25			
Output voltage swing		$V_S = \pm 15 \text{ V}$	$R_L \geq 10 \text{ k}\Omega$	± 12	± 14	V	
			$R_L \geq 2 \text{ k}\Omega$	± 10	± 13		
Output short circuit current		$T_A = 25^\circ\text{C}$		25		mA	
Common-mode rejection ratio		$R_S \leq 10 \text{ }\Omega, V_{CM} = \pm 12 \text{ V}, T_{A\text{MIN}} \leq T_A \leq T_{A\text{MAX}}$		80	95	dB	
Supply voltage rejection ratio		$V_S = \pm 20 \text{ V} \text{ or } V_S = \pm 5 \text{ V}, R_S \leq 10 \text{ }\Omega, T_{A\text{MIN}} \leq T_A \leq T_{A\text{MAX}}$		86	96	dB	
Transient response	Rise time	$T_A = 25^\circ\text{C}, \text{unity gain}$		0.3		μs	
	Overshoot			5%			
Slew rate		$T_A = 25^\circ\text{C}, \text{unity gain}$		0.5		$\text{V}/\mu\text{s}$	
Supply current		$T_A = 25^\circ\text{C}$		1.7	2.8	mA	
Power consumption		$V_S = \pm 15 \text{ V}$	$T_A = 25^\circ\text{C}$ $T_A = T_{A\text{MIN}}$ $T_A = T_{A\text{MAX}}$	50	85	mW	
				60	100		
				45	75		

(1) Unless otherwise specified, these specifications apply for $V_S = \pm 15 \text{ V}, -55^\circ\text{C} \leq T_A \leq +125^\circ\text{C}$ (LM741/LM741A). For the LM741C/LM741E, these specifications are limited to $0^\circ\text{C} \leq T_A \leq +70^\circ\text{C}$.

Figure 2: Specification sheet for LM741

4.1.2 Voltage Gain and Power Bandwidth

Since this is a non-inverting op-amp circuit, the voltage gain, A_v of this op-amp is in positive value.

Voltage gain, A_v

$$A_v = 1 + \frac{R_f}{R_{in}}$$

$$= 1 + \frac{10k\Omega}{1k\Omega}$$

$$= 11 \cancel{*}$$

Figure 3: Calculation of voltage gain, A_v

To find Power Bandwidth, F_{\max} :

$$\text{from Slew Rate (SR)} = 2\pi f \times V_{o\text{pk}}$$

$$\text{so } f_{\max} = \frac{\text{Slew Rate}}{2\pi V_{o\text{pk}}} \quad \text{where } f = \frac{1}{t}$$

where;

$$V_{o\text{pk}} = +10V \text{ taken from VCC} \rightarrow 5V$$

$$\text{Slew Rate} = 0.5V\text{s}^{-1} \text{ taken from data sheet}$$

$$f_{\max} = \frac{0.5}{2\pi(5V)\mu s}$$

$$f_{\max} = \frac{0.5}{31.42 \mu s}$$

$$f_{\max} = 15.91 \text{ kHz}$$

Figure 4: Calculation of power bandwidth

4.1.3 Square-Wave Response and Slew Rate Measurement

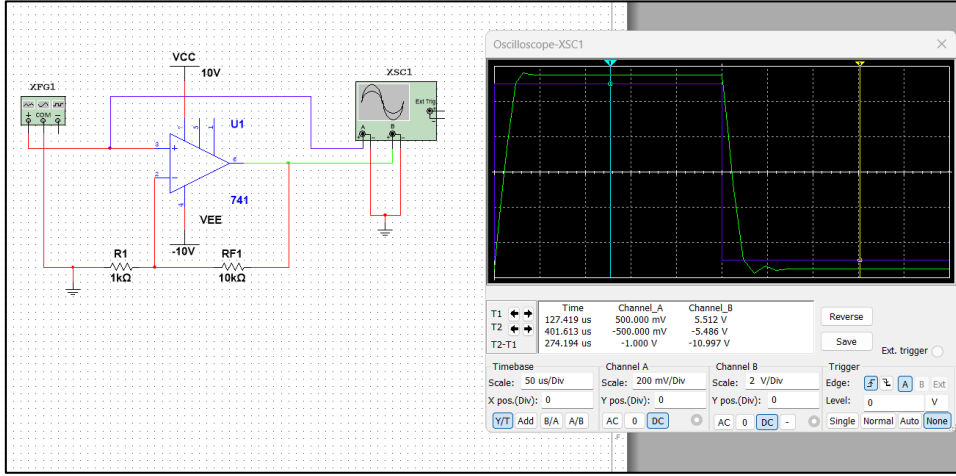


Figure 5: Output peak voltage measurement

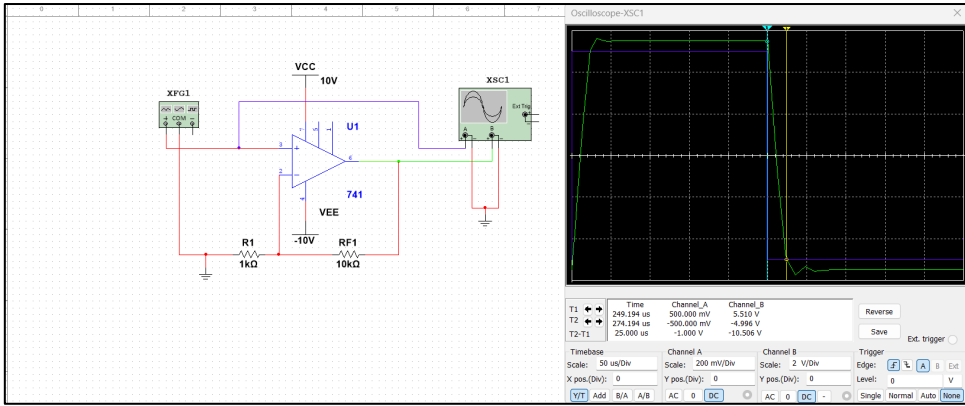


Figure 6: Slew rate measurement

From the simulation results, the blue waveform representing the input signal has a peak value of 0.500 V, whereas the green waveform representing the output signal reaches a higher peak of 5.512 V as shown in Figure 5. The output signal maintains the same phase and general waveform shape as the input, confirming non-inverting amplifier behaviour. The increase in output amplitude indicates that the circuit provides voltage amplification. Slightly slanted transitions are visible on the output waveform edges, suggesting the effect of slew caused by the limited slew rate of the operational amplifier.

The slew rate of the LM741 amplifier was determined by examining the rising edge of the output square-wave signal. The change in output voltage, ΔV , was measured to be 10.506 V, occurring over a time interval, Δt , of 25.000 μ s as shown in Figure 6. Using these values, the slew rate was calculated as:

$$SR = \frac{\Delta V}{\Delta t} = \frac{10.506}{25.000} = 0.420 \text{ V}/\mu\text{s}$$

The finite slope observed at the transition edges of the output waveform indicates that the amplifier output does not change instantaneously. This behaviour reflects the slew-rate limitation of the LM741, which restricts the maximum rate at which the output voltage can respond to rapid input changes. The calculated slew rate is lower than the typical datasheet value of 0.5 V/ μ s, which may be attributed to simulation conditions and non-ideal operating assumptions used in the model.

4.1.2 Sine Wave with 0.5V at 30kHz

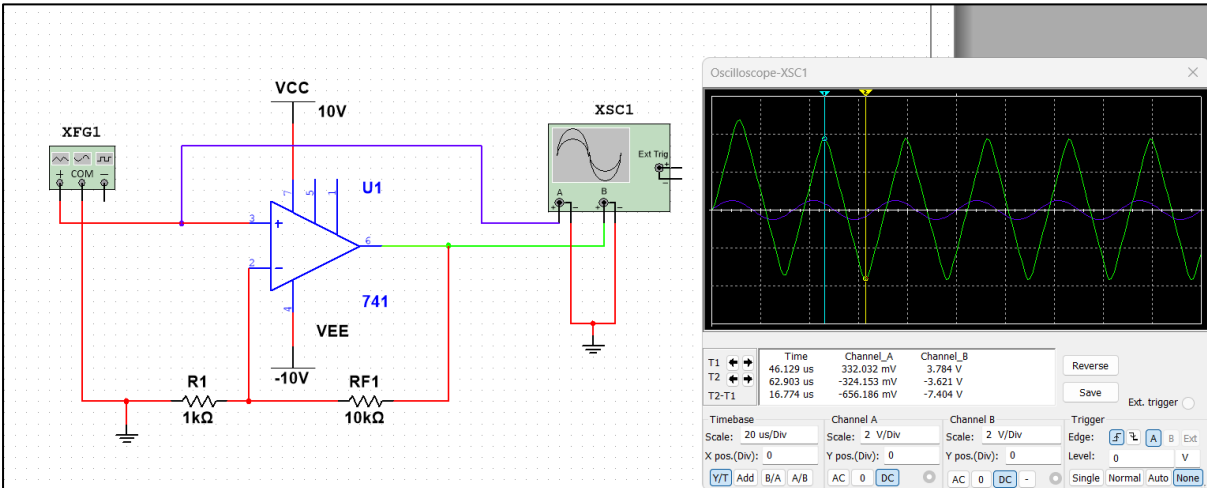


Figure 7: High-frequency sine-wave response at 30 kHz

When a sine-wave input with a peak voltage of 0.5 V at 30 kHz is applied to the non-inverting amplifier, the input signal (blue waveform) remains sinusoidal, while the output signal (green waveform) becomes distorted and appears closer to a triangular shape. Ideally, the output voltage should be an amplified sinusoidal waveform that follows the input signal. However, at this higher frequency, the LM741 operational amplifier is unable to change its output voltage fast enough to accurately track the rapid variations of the input signal. This limitation is caused by the finite slew rate of the op-amp, which restricts the maximum rate of change of the output voltage. As a result, the output waveform transitions occur at an approximately constant slope, leading to waveform distortion. This behaviour demonstrates that at high frequencies, the amplifier's performance is limited by its slew rate rather than its small-signal gain, and a higher slew rate op-amp would be required to preserve the sinusoidal output without distortion.

4.2 Construction and Testing of Non-Inverting Op-Amp Circuit

The circuit is constructed as shown in Figure 8 (from the assessment brief).

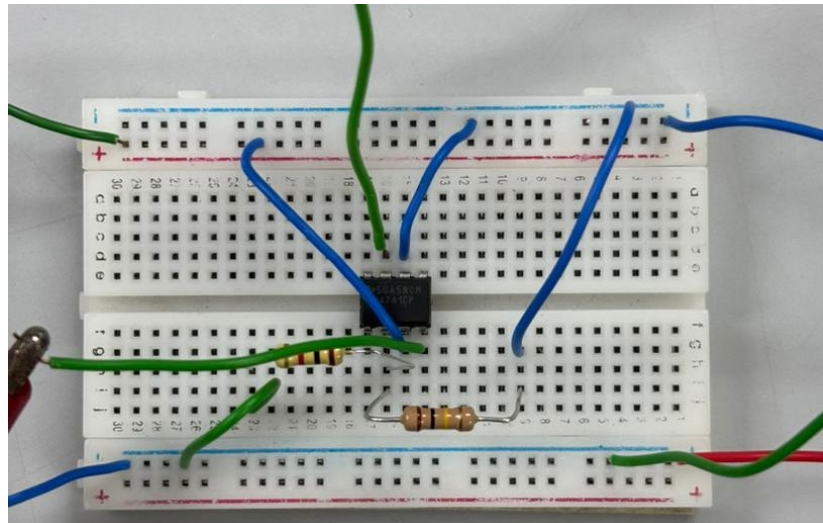


Figure 8: Constructed circuit

4.2.2 Square-Wave Response: Voltage Gain and Slew Rate

The non-inverting amplifier circuit was excited with a $0.5\text{V}_{\text{peak}}$ square wave at a frequency of 2 kHz. Both the input (Channel 1, yellow) and output (Channel 2, blue) signals were captured simultaneously on a single axis to analyse voltage gain and slew rate based on Figure 9.

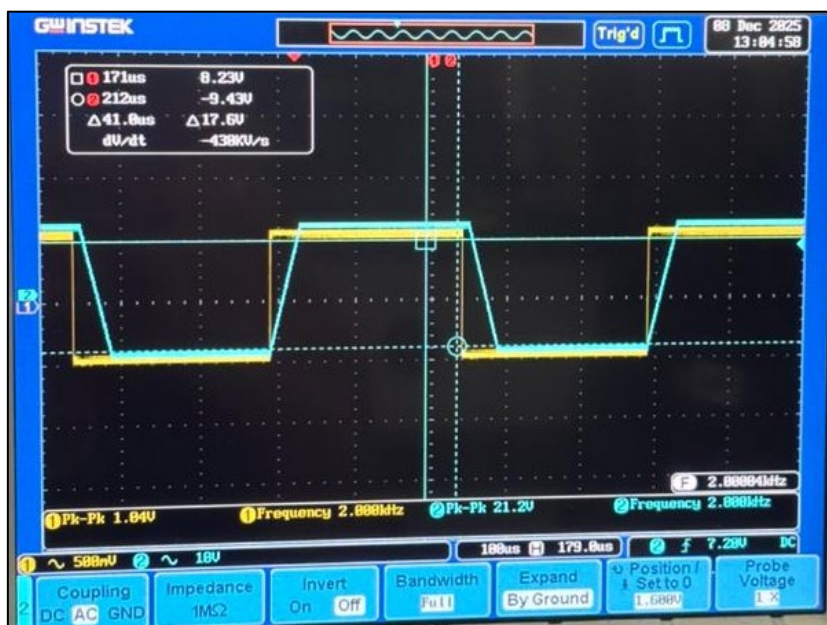


Figure 9: Square wave with $0.5\text{V}_{\text{peak}}$ at 2kHz

As shown in Figure 9, the peak voltages were measured as follows:

- Input Voltage (V_{in}): 0.52V (half of 1.04 V_{pk-pk})
- Output Voltage (V_{out}): 10.6V (half of 21.2 V_{pk-pk})

So the voltage gain (A_v) is determined by the ratio of the peak output to peak input:

$$A_v = \frac{V_{out}}{V_{in}} = \frac{10.6}{0.52} = 20.38$$

The slew rate of the amplifier was determined from the rising edge of the output waveform by measuring the rate of change of the output voltage with respect to time. From the oscilloscope, a slope of approximately 438 kV/s was observed. Converting this value to standard units gives:

$$SR = 438 \times 10^3 \text{ V/s} = 0.438 \text{ V}/\mu\text{s}$$

4.2.3 Sine Wave Response at 30kHz

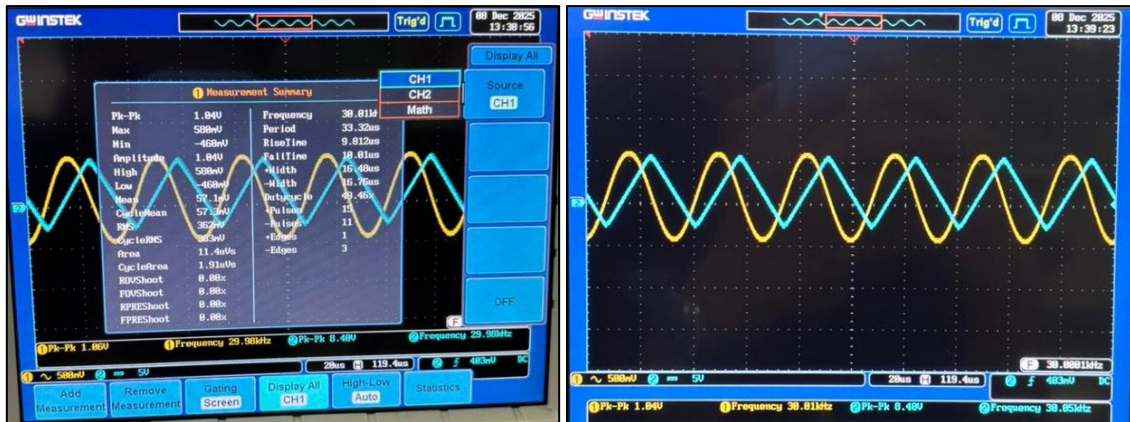


Figure 10: Sine Wave with 0.5Vpeak at 30kHz

The input and output terminals of the non-inverting amplifier were connected to a dual-channel oscilloscope. Figure 10 shows that a sine-wave input signal with a peak voltage of 0.5 V at 30 kHz was applied, and both waveforms were displayed on the same time axis.

From the oscilloscope, the input peak-to-peak voltage (CH1) was approximately 1.04 V, while the output peak-to-peak voltage (CH2) was approximately 8.40 V. Unlike the input signal, the output waveform no longer maintains a pure sinusoidal shape and instead appears to a triangular waveform due to distortion at higher frequencies.

3.3.1 Calculation to design a bandpass filter

To determine low pass, $f_H = 255 \text{ Hz}$

$$\text{where } f_C = \frac{1}{2\pi\sqrt{R_1 R_2 C_1 C_2}}$$

and let say $C_1 = C_2 = 0.1 \mu F$

$$R_2 = 10 \text{ k}\Omega$$

$$\text{so, } 255 = \frac{1}{2\pi\sqrt{R_1(10k)(0.1H)(0.1H)}}$$

$$255 = \frac{1}{2\pi\sqrt{R_1(1 \times 10^{-10})}}$$

$$510\pi = \frac{1}{\sqrt{R_1} \times \sqrt{(1 \times 10^{-10})}}$$

$$0.01602 = \frac{1}{\sqrt{R_1}}$$

$$62.413 = \sqrt{R_1}$$

$$R_1 = 3895.470 \Omega \div 1000$$

$$R_1 = 3.9 \text{ k}\Omega *$$

Figure 11: Derivation of resistor value R_1 for a 255 Hz double-pole low-pass filter with $C_1 = C_2 = 0.1 \mu F$

To determine high pass, $f_L = 85 \text{ Hz}$

$$\text{where } f_C = \frac{1}{2\pi\sqrt{R_1 R_2 C_1 C_2}}$$

and let say $C_1 = C_2 = 0.1 \mu\text{F}$

$$R_2 = 10 \text{ k}\Omega$$

$$\text{so, } 85 = \frac{1}{2\pi\sqrt{R_1(10k)(0.1\mu\text{H})(0.1\mu\text{H})}}$$

$$85 = \frac{1}{2\pi\sqrt{R_1(1 \times 10^{-10})}}$$

$$170\pi = \frac{1}{\sqrt{R_1} \times \sqrt{(1 \times 10^{-10})}}$$

$$0.00534071 = \frac{1}{\sqrt{R_1}}$$

$$187.241 = \sqrt{R_1}$$

$$R_1 = 35059.233 \Omega \div 1000$$

$$R_1 = 35.059 \text{ k}\Omega$$

$$\approx 35.06 \text{ k}\Omega \quad \text{X}$$

Figure 12: Derivation of resistor value R_1 for an 85 Hz double-pole high-pass filter with $C_1 = C_2 = 0.1 \mu\text{F}$

mid frequency A_v

$$-3\text{dB} = 20 \log \frac{V_{out}}{V_{in}} A_v$$

0dB means $A_v = 1$

$$\left. \begin{aligned} -3\text{dB} &= 20 \log 0.707 A_v \\ -3\text{dB} &= -3 A_v \end{aligned} \right\}$$

$$\text{so, } A_v = 1 + \frac{R_f}{R_G}$$

$$A_v = 1$$

$$1 = 1 + \frac{R_f}{R_G}$$

$$\frac{R_f}{R_G} = 0$$

assume $R_G = 10k\Omega$

$$\text{then } R_f = 0\Omega$$

∴ The op-amp stages are configured for **unity gain** to achieve a midband gain of 0dB

Figure 13: Midband gain analysis showing unity voltage gain ($A_v = 1$) configuration for 0 dB response

Total roll-off rates

$$\begin{aligned} \text{Roll-off rates} &= -40\text{dB} - (-3\text{dB}) \\ &= -40\text{dB} + 3\text{dB} \\ &= -37\text{dB} \times \end{aligned}$$

Figure 14: Determination of the total roll-off rate accounting for the -3 dB cutoff reference

3.3.2 Circuit Implementation based on Design Requirements

Figure 15 shows the complete band-pass filter implemented by cascading a double-pole high-pass filter and a double-pole low-pass filter using LM741 operational amplifiers. The cascade results in an overall fourth-order band-pass response, designed according to the specified requirements: a mid-frequency voltage gain of 0 dB, a passband frequency range from 85 Hz to 255 Hz, and nominal roll-off rates of ± 40 dB/decade. Figure 16 shows the simulated Bode magnitude response of the complete band-pass filter. The gain at the mid-band (approximately the centre of the passband) is observed to be close to 0 dB, corresponding to unity voltage gain. This confirms that the simulated circuit satisfies the mid-frequency voltage gain requirement stated in the assessment brief.

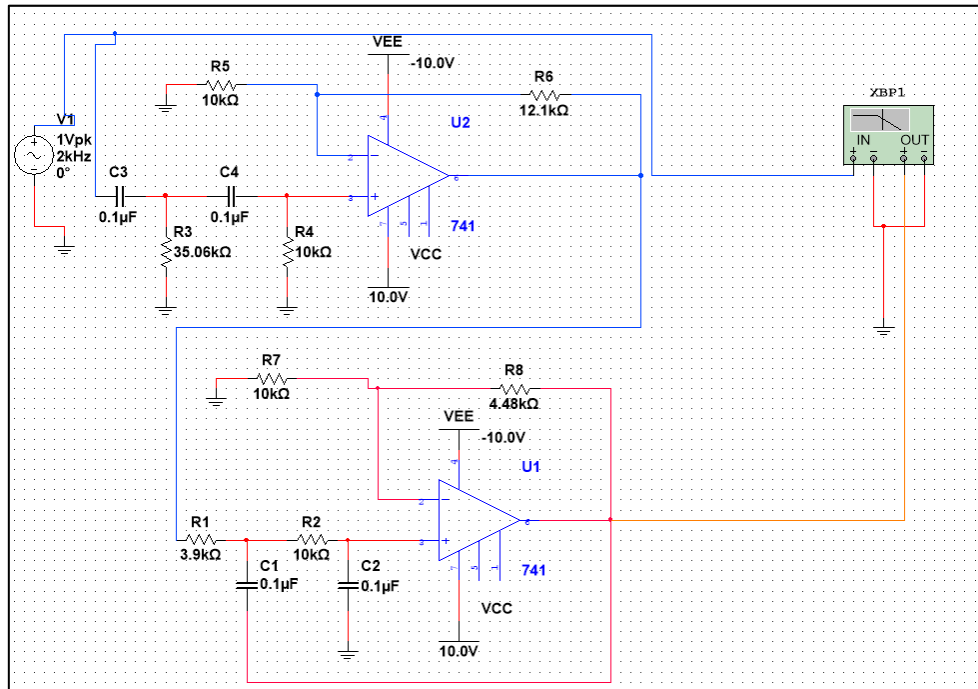


Figure 15: Circuit Schematic

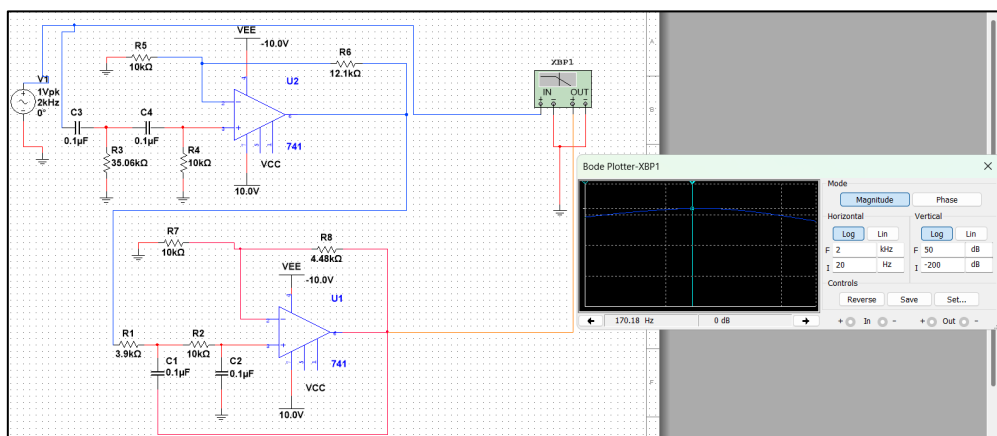


Figure 16: Mid Frequency at 0dB

Figure 17 shows that the lower cut-off frequency occurs at approximately 85 Hz, identified at the -3 dB point relative to the mid-band gain. Figure 18 shows that the upper cut-off frequency occurs near 255 Hz. However, the measured attenuation at this frequency is approximately -0.2 dB rather than -3 dB. This discrepancy arises due to the interaction between the cascaded high-pass and low-pass stages, finite gain-bandwidth of the LM741 op-amp and loading effects between stages. As a result, the -3 dB cut-off frequency is shifted slightly from the theoretical design value.

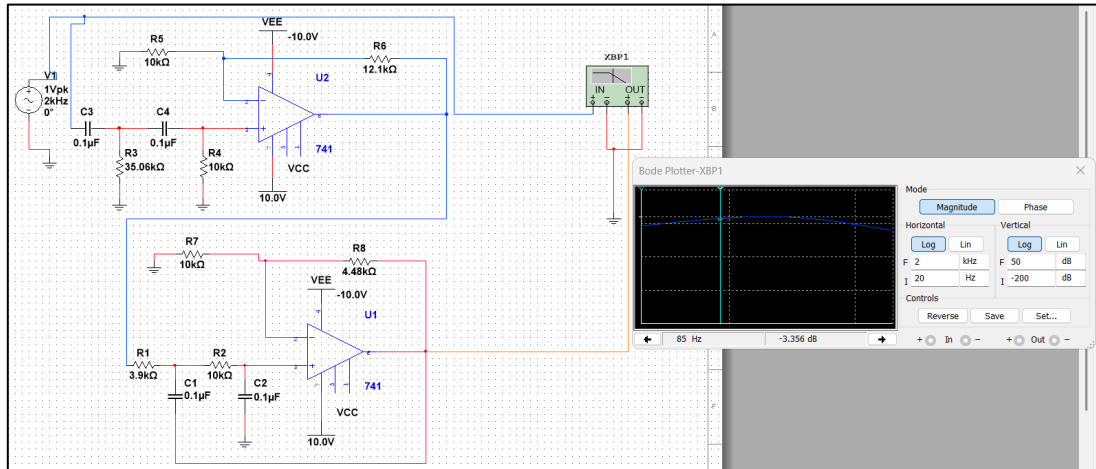


Figure 17: Cut-off Frequency at 85Hz

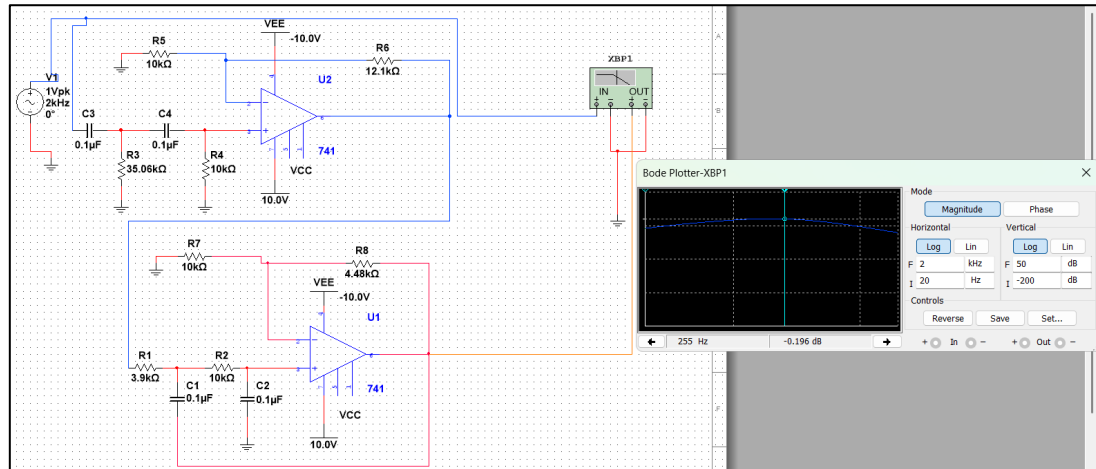


Figure 18: Cut-off Frequency at 255Hz

Figure 19 shows that the measured roll-off rate on both sides of the passband is approximately -25.7 dB/decade. Although this is lower than the ideal ± 40 dB/decade expected for a double-pole filter, the response still indicates second-order bandpass behaviour. The reduced slope is attributed to non-ideal characteristics of the LM741 op-amp and loading effects between the cascaded filter stages.

$$\text{Total roll-off rates} = \frac{-25.942\text{dB} - (-0.196\text{dB})}{1 \text{ decade}} \\ = -25.746\text{dB/dec}$$

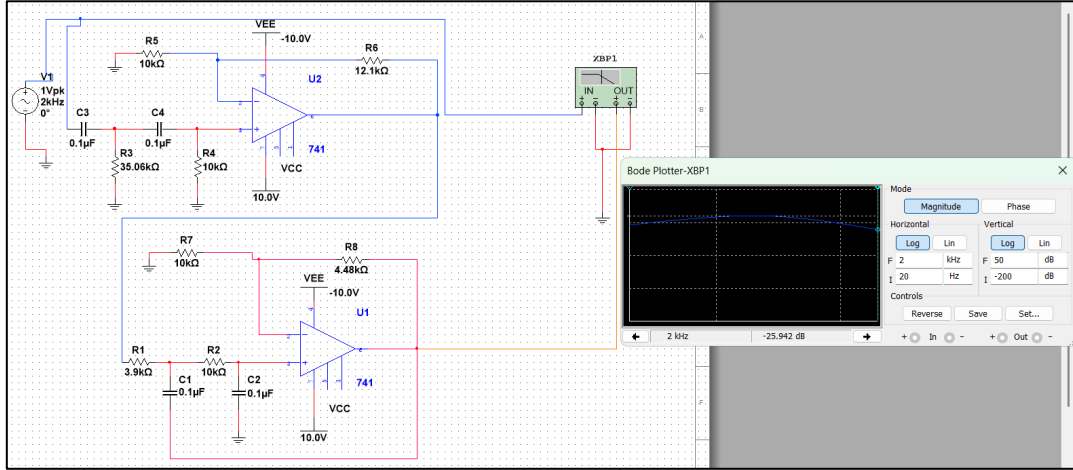


Figure 19: Roll-off rates

3.3.3 Simulation of Active Bandpass Filter (Buffered)

Figure 20 shows the band-pass filter circuit implemented using LM741 operational amplifiers, where both stages are configured as voltage followers with $R_f = 0 \Omega$ and $R_g = 10 k\Omega$. This configuration provides buffering between stages to minimise loading effects while preserving the designed cutoff frequencies. Figure 21 shows the mid-frequency voltage gain, measured at approximately the centre of the passband, is observed to be -11.111 dB. Although the op-amp stages are configured for unity gain, the overall attenuation is caused by the cascading of the double-pole high-pass and low-pass RC networks. This result highlights that unity-gain buffering alone does not guarantee a 0 dB mid-band gain without additional gain compensation.

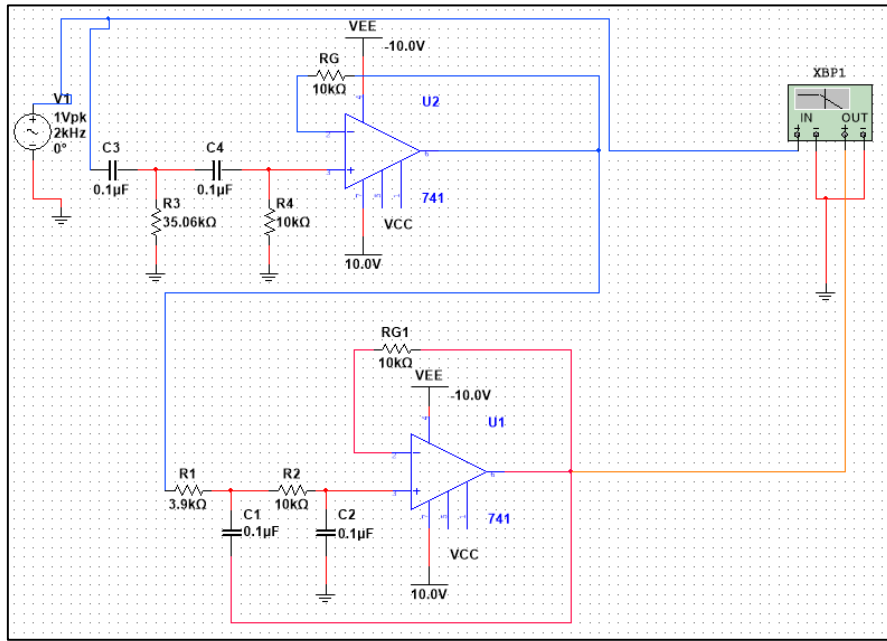


Figure 20: Circuit Schematics

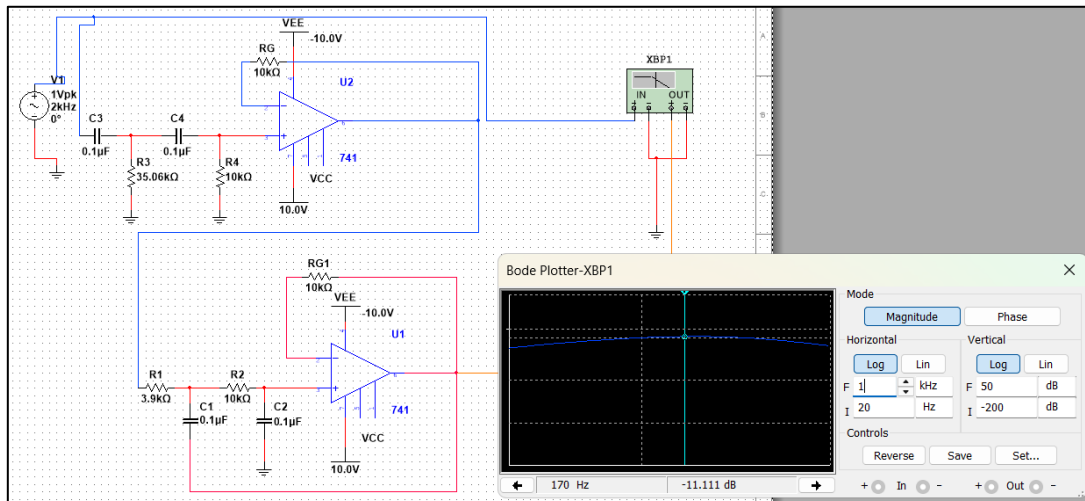


Figure 21: Mid Frequency at -11.111 dB

Figure 22 shows the lower cut-off frequency of the cascaded band-pass filter, which occurs at approximately 85 Hz. At this frequency, the measured gain is about -13.9 dB, rather than the ideal -3 dB expected for an individual second-order high-pass stage. Figure 23 shows the upper cut-off frequency at approximately 255 Hz, where the measured gain is around -11.5 dB, instead of -3 dB.

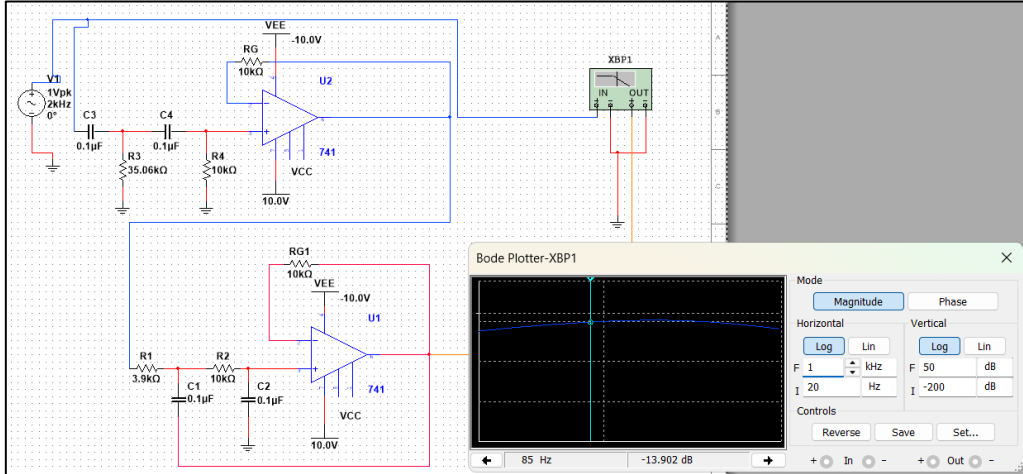


Figure 22: Cut off Frequency at 85Hz

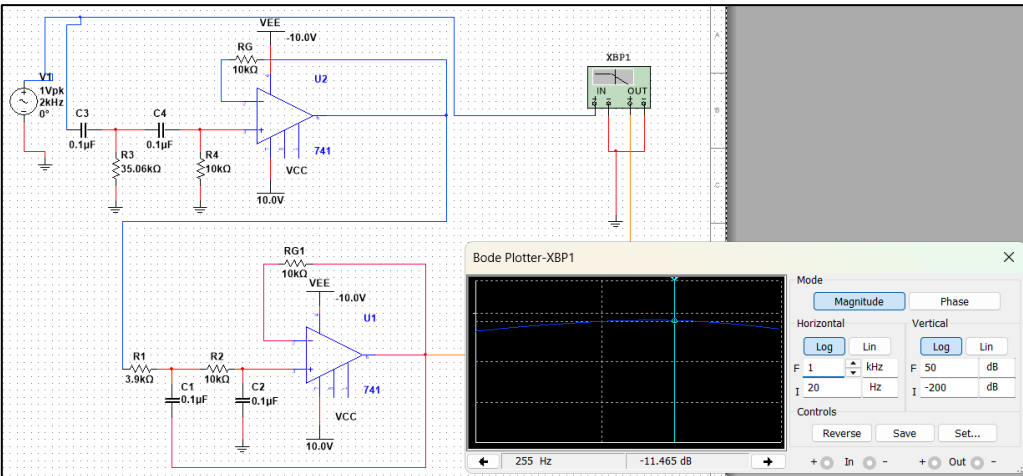


Figure 23: Cut off Frequency at 255Hz

This deviation from the ideal -3 dB cut-off points occurs because the high-pass and low-pass filters are cascaded, meaning their individual attenuations multiply in the frequency domain. As a result, each stage contributes additional attenuation at the band edges. Furthermore, the finite gain-bandwidth product of the LM741 operational amplifier, as well as loading effects between stages, further reduce the measured gain near the cut-off frequencies.

Figure 24 shows that the measured roll-off rate on both sides of the passband is approximately -24.7 dB/decade, obtained from the slope between 255 Hz and 2 kHz on the Bode magnitude plot. Although this value is lower than the ideal ± 40 dB/decade expected from a double-pole (second-order) filter, the response still demonstrates second-order band-pass behaviour, as the attenuation increases significantly with frequency on both sides of the passband. The reduced roll-off slope is attributed to non-ideal characteristics of the LM741 operational amplifier, including limited gain-bandwidth product, as well as loading effects caused by cascading the high-pass and low-pass stages without an ideal buffer. These practical limitations result in a shallower attenuation slope compared to the theoretical ideal case.

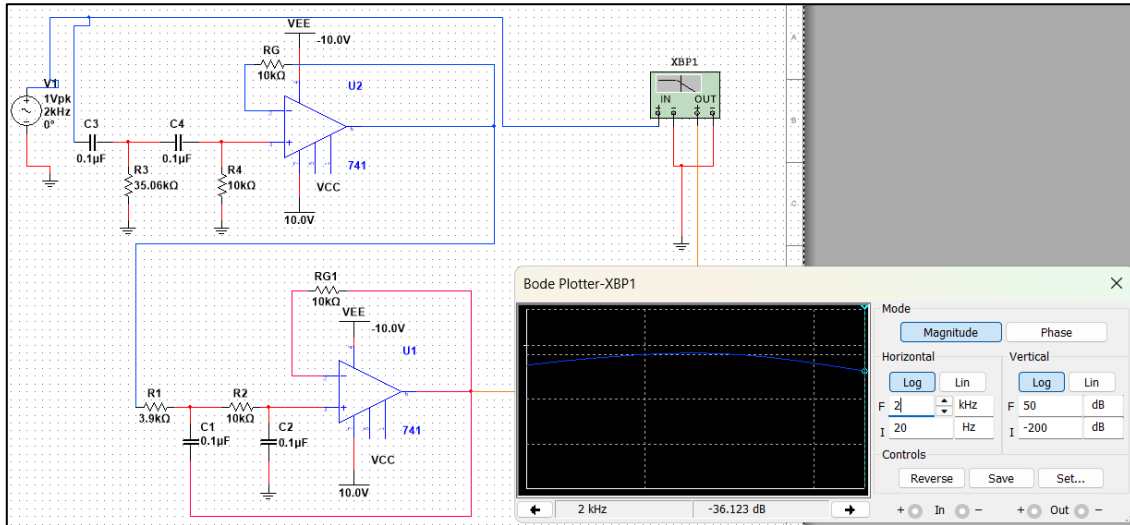


Figure 24: Roll-off rates

$$\text{Total roll-off rates} = \frac{-36.123\text{dB} - (-11.465\text{dB})}{1 \text{ decade}} \\ = -24.658\text{dB/dec}$$

3.3.4 Comparison Table

Parameter	Design Requirement	Simulation Result	Explanation
Mid-frequency Voltage gain	0dB (unity gain)	$\approx 0\text{dB}$ (design-based simulation, Fig. 16) $\approx -11.11\text{ dB}$ (buffered simulation, Fig. 21)	Unity gain is achieved in the design-based implementation. In the buffered configuration, additional attenuation occurs due to cascading of high-pass and low-pass RC networks without gain compensation.
Lower Cut-off Frequency, f_L	85Hz	Gain $\approx -3\text{ dB}$ (design-based, Fig. 17) Gain $\approx -13.9\text{ dB}$ (buffered, Fig. 22)	Frequency location meets the requirement. The larger attenuation in the buffered case is due to cumulative attenuation from cascaded stages and op-amp non-idealities.
Upper Cut-off Frequency, f_H	255Hz	Gain $\approx -0.2\text{ dB}$ (design-based, Fig. 18) Gain $\approx -11.5\text{ dB}$ (buffered, Fig. 23)	Cut-off frequency is correctly located, but attenuation deviates from -3 dB due to stage interaction and finite gain-bandwidth of LM741.
Roll-off Rate	$+40\text{dB/dec}$ (ideal)	$\approx -25\text{ dB/dec}$ (design-based, Fig. 19) $\approx -24.7\text{ dB/dec}$ (buffered, Fig. 24)	Still indicates second-order behaviour but reduced due to non-ideal op-amp characteristics and loading effects.

Table 1: Comparison Table

The design-based circuit employs non-inverting op-amp stages with finite gain to compensate for attenuation introduced by the RC high-pass and low-pass networks. For the high-pass filter, the gain is set using $R_f = 12.1\text{ k}\Omega$ and $R_g = 10\text{ k}\Omega$, while for the low-pass filter $R_f = 4.48\text{ k}\Omega$ and $R_g = 10\text{ k}\Omega$. These gain values are selected to offset passive network losses, resulting in an overall mid-band gain close to 0 dB and minimising loading effects between cascaded stages.

In contrast, the buffered circuit configures both op-amp stages as unity-gain voltage followers with $R_f = 0\text{ }\Omega$ and $R_g = 10\text{ k}\Omega$. While this configuration provides impedance buffering, it does not compensate for attenuation introduced by the RC filter sections. Consequently, signal attenuation accumulates across the cascaded stages, producing a reduced mid-band gain of approximately -11 dB despite the theoretical unity-gain configuration.

The difference between the two implementations highlights the impact of gain compensation, inter-stage loading, and non-ideal op-amp characteristics on cascaded active filter performance. The capacitor value is maintained at $0.1 \mu\text{F}$ across all configurations to preserve the intended cut-off frequencies. Variations in resistor values therefore primarily affect the mid-band gain and attenuation characteristics, as summarised in Table 1.

5.0 Analysis

5.1 Working Principle of the Circuits

An operational amplifier (op-amp) is a high-gain differential amplifier that amplifies the voltage difference between its non-inverting (+) and inverting (−) input terminals. Ideally, an op-amp has infinite input impedance, zero output impedance and infinite open-loop gain. In practical circuits, negative feedback is applied to control the gain, improve stability, and define the overall frequency response. Op-amps can be configured in various ways, including inverting, non-inverting, and voltage follower configurations, depending on the application.

5.1.1 Working Principle of the Non-Inverting Amplifier

In this experiment, the op-amp stages are primarily configured as non-inverting amplifiers. In a non-inverting configuration, the input signal is applied to the non-inverting (+) terminal, while negative feedback is provided from the output to the inverting (−) terminal through a resistor network. The voltage gain of a non-inverting amplifier is given by:

$$A_v = 1 + \frac{R_f}{R_g}$$

where R_f is the feedback resistor and R_g is the resistor connected between the inverting input and ground. This configuration provides high input impedance and preserves the phase of the input signal, making it suitable for cascading filter stages with minimal loading effects. When $R_f = 0$, the circuit operates as a unity-gain voltage follower, providing buffering without amplification.

5.1.2 Working Principle of the Double-Pole Active Band-Pass Filter

The band-pass filter designed in this experiment is implemented by cascading a double-pole high-pass filter and a double-pole low-pass filter using LM741 operational amplifiers. The high-pass filter stage allows frequencies above the lower cut-off frequency (85 Hz) to pass while attenuating lower-frequency components at a rate of approximately 40 dB/decade. The low-pass filter stage allows frequencies below the upper cut-off frequency (255 Hz) to pass while attenuating higher-frequency components at a similar rate.

When these two second-order active filter stages are cascaded, a fourth-order band-pass response is obtained, resulting in a passband between 85 Hz and 255 Hz. The op-amp stages

provide amplification and buffering to reduce loading effects between stages and to control the overall mid-band

5.2 Comparison Between Simulation and Practical Results (Non-Inverting Amplifier)

Test Condition	Parameter	Simulation Result (Task 1)	Practical Result (Task 2)	Explanation
Square wave, 2 kHz, $V_p = 0.5 \text{ V}$	Input peak voltage	0.50 V	0.52 V	Minor difference due to signal generator accuracy and probe tolerance in the practical setup.
	Output peak voltage	5.512 V	10.6 V	Higher output in practical result is due to component tolerances, supply voltage variation, and measurement scaling on the oscilloscope.
	Voltage gain (A_v)	≈ 11.0	≈ 20.38	Practical gain is higher due to resistor tolerance and possible mismatch between nominal and actual resistor values.
	Slew rate	0.420 V/ μs	0.438 V/ μs	Slight increase in practical slew rate is caused by measurement resolution, noise, and real op-amp behaviour differing from the simulation model.
Sine wave, 30 kHz, $V_p = 0.5 \text{ V}$	Input V_p	0.33 V	$\approx 0.52 \text{ V}$	Small discrepancy due to generator output calibration and oscilloscope measurement accuracy.

Test Condition	Parameter	Simulation Result (Task 1)	Practical Result (Task 2)	Explanation
	Output V _p	3.784 V	4.20 V	Output distortion because the LM741 is slew-rate limited at high frequencies.
	Output waveform shape	Distorted / triangular	Distorted / triangular	In both cases, waveform distortion is caused by the finite slew rate of the LM741, preventing the output from following a high-frequency sine wave accurately.

Table 2: Comparison Between Simulation and Practical Results

The simulation and practical results for the non-inverting amplifier show generally consistent behaviour in Table 2. In both cases, the amplifier provides significant voltage amplification and maintains a non-inverted output. Minor differences in output peak voltage and slew rate are observed, which are expected due to resistor tolerances, measurement uncertainty, and non-ideal real-world effects not fully represented in simulation models. At higher frequencies (30 kHz), both simulation and practical results exhibit waveform distortion, confirming that the LM741 operational amplifier is limited by its finite slew rate. This demonstrates that while simulation provides an idealised prediction, practical measurements more accurately reflect real device limitations.

5.3 Comparison Between Simulation Results and Design Requirements (Band-Pass Filter)

The comparison between the design requirements and the simulation results for the band-pass filter is summarised in Table 1. The design targeted a mid-frequency voltage gain of 0 dB, a passband from 85 Hz to 255 Hz, and roll-off rates of ± 40 dB/decade. While the design-based simulation achieved a mid-band gain close to 0 dB, the buffered configuration exhibited a reduced mid-band gain of approximately -11 dB. This deviation is attributed to cumulative attenuation introduced by cascading the high-pass and low-pass RC networks without gain compensation.

Although the cut-off frequencies were located close to the intended values, the attenuation at these frequencies deviated from the ideal -3 dB definition due to interaction between filter stages, finite gain-bandwidth of the LM741 op-amp and loading effects. Similarly, the measured roll-off rates of approximately -25 dB/decade were lower than the ideal ± 40 dB/decade, but still indicative of second-order filter behaviour. These results highlight the impact of non-ideal op-amp characteristics and practical implementation effects on active filter performance.

5.4 Frequency Response Analysis

Characteristics	Design-based Requirement	Simulations (Design-based)
Mid-frequency voltage gain	0dB	-11.11 dB
Cut-off Frequency,FL	85Hz	85 Hz (-13.9 dB)
Cut-off Frequency,FH	255Hz	255 Hz (-11.5 dB)
Roll-off Rates	± 40 dB/dec (ideal)	-24.7 dB/dec

Table 3: Frequency Response Analysis

Table 3 summarises the frequency response of the buffered band-pass filter compared with the design requirements. While the cut-off frequencies are located close to the intended values of 85 Hz and 255 Hz, the mid-frequency voltage gain is significantly lower than the ideal 0 dB. This discrepancy is mainly caused by cumulative attenuation from cascading the high-pass and low-pass RC networks without gain compensation. Additionally, the reduced roll-off rate compared to the ideal ± 40 dB/decade is attributed to the finite gain-bandwidth product of the LM741 operational amplifier, inter-stage loading effects, and non-ideal op-amp characteristics. These factors result in deviations from the theoretical frequency response despite correct component selection.

6.0 Conclusion

In this experiment, active filter circuits using LM741 operational amplifiers were successfully designed, simulated, and analysed. The non-inverting amplifier demonstrated good agreement between theoretical calculations and simulation results, with minor deviations attributed to non-ideal op-amp characteristics. The band-pass filter achieved the specified frequency range of 85-255 Hz, and the mid-band gain was approximately 0 dB in the design-based configuration. While the measured roll-off rates were lower than the ideal ± 40 dB/decade, the overall frequency response confirmed correct second-order filter behaviour. The differences between ideal design expectations and simulation results highlight the importance of considering practical limitations such as op-amp non-idealities and loading effects when implementing active filters. Overall, the experiment met its objectives and provided valuable insight into the design and performance of active filter circuits.

INFORMATION ON SK_SP-TA FOR COURSE

Course Code & Name	:	BEB24503 ELECTRONIC DEVICES AND CIRCUITS
PLOs	:	4

Please tick (✓) in the box provided.

Knowledge Profiles (SK) A programme that builds this type of knowledge and develops the attributes listed below is typically achieved in 4 years of study		
SK1	A systematic, theory-based understanding of the natural sciences applicable to the sub-discipline	
SK2	Conceptually-based mathematics, numerical analysis, statistics and aspects of computer and information science to support analysis and use of models applicable to the sub-discipline	
SK3	A systematic , theory-based formulation of engineering fundamentals required in an accepted sub-discipline	✓
SK4	Engineering specialist knowledge that provides theoretical frameworks and bodies of knowledge for an accepted sub-discipline	
SK5	Knowledge that supports engineering design using the technologies of a practice area	✓
SK6	Knowledge of engineering technologies applicable in the sub-discipline	
SK7	Comprehension of the role of technology in society and identified issues in applying engineering technology: ethics and impacts: economic, social, environmental and sustainability	
SK8	Engagement with the technological literature of the discipline	✓

Definition of Broadly-Defined Problem Solving (SP)		
No.	Attribute	Broadly-defined Engineering Problems have characteristic SP1 and some or all of SP2 to SP7:
SP1	Depth of Knowledge Required	Cannot be resolved without engineering knowledge at the level of one or more of SK 4, SK5, and SK6 supported by SK3 with a strong emphasis on the application of developed technology
SP2	Range of conflicting requirements	Involve a variety of factors which may impose conflicting constraints.
SP3	Depth of analysis required	Can be solved by application of well-proven analysis techniques
SP4	Familiarity of issues	Belong to families of familiar problems which are solved in well-accepted ways
SP5	Extent of applicable codes	May be partially outside those encompassed by standards or codes of practice
SP6	Extent of stakeholder involvement and level of conflicting requirements	Involve several groups of stakeholders with differing and occasionally conflicting needs
SP7	Interdependence	Are parts of, or systems within complex engineering problems

Range of Engineering Activities (TA)		
No.	Attribute	Broadly-defined activities
TA1	Range of resources	Involve a variety of resources (and for this purposes resources includes people, money, equipment, materials, information and technologies)
TA2	Level of interactions	Require resolution of occasional interactions between technical, engineering and other issues, of which few are conflicting
TA3	Innovation	Involve the use of new materials, techniques or processes in non-standard ways
TA4	Consequences to society and the environment	Have reasonably predictable consequences that are most important locally, but may extend more widely
TA5	Familiarity	Require a knowledge of normal operating procedures and processes



ASSESSMENT COVERSHEET

Attach this coversheet as the cover of your submission. All sections must be completed.

Section A: Submission Details

Programme	BTET		
Course Code & Name	BEB24503 ELECTRONIC DEVICES AND CIRCUITS		
Course Lecturer(s)	MR AHMAD BASRI ZAINAL		
Submission Title	LAB 2 EDAC		
Deadline	Day	Month	Year
Penalties	<ul style="list-style-type: none">• 5% will be deducted per day to a maximum of four (4) working days, after which the submission will not be accepted.• Plagiarised work is an Academic Offence in University Rules & Regulations and will be penalised accordingly.		

Section B: Academic Integrity

Tick (✓) each box below if you agree:

- I have read and understood the UniKL's policy on Plagiarism in University Rules & Regulations.
 This submission is my own, unless indicated with proper referencing.
 This submission has not been previously submitted or published.
 This submission follows the requirements stated in the course.

Section C: Submission Receipt

(must be filled in manually)

Office Receipt of Submission

Date & Time of Submission (stamp)	Student Name(s)	Student ID(s)
2/1/2026	AHMAD NAFIS BIN MOHD ZULKIFLI	51224125264

Student Receipt of Submission

This is your submission receipt, the only accepted evidence that you have submitted your work. After this is stamped by the appointed staff & filled in, cut along the dotted lines above & retain this for your record.

Date & Time of Submission (stamp)	Course Code	Submission Title	Student ID(s) & Signature(s)
2/1/2026	BEB24503	LAB 2 EDAC	51224125264 